INT. J. REMOTE SENSING, 10–20 APRIL, 2004,
VOL. 25, NO. 7–8, 1331–1336

Using sea surface temperature measurements from microwave and infrared satellite measurements

C. J. DONLON*†, L. NYKJAER† and C. GENTEMANN‡

†European Commission Joint Research Centre, Institute for Environment and Sustainability, Ispra, 21020, Italy
‡Remote Sensing Systems, 438 First St., Suite 200, Santa Rosa, CA 95401, USA

Abstract. The Tropical Rainfall Mapping Mission Microwave Imager (TMI) instrument Sea Surface Temperature (SST) product (v1.0) is compared with *in situ* observations obtained in the Atlantic Ocean. The TMI SST has a mean warm bias of $0.25\,K \pm 0.7\,K$ when compared to *in situ* SST at a depth of 7 m. When TMI SST are compared to *in situ* skin SST measurements, the bias is $0.6\,K \pm 0.5\,K$. A limited global comparison between TMI SST and co-incident ERS-2 Along-Track Scanning Radiometer (ATSR/2) skin SST demonstrates a bias of $0.6\,K \pm 0.6\,K$ consistent with the result obtained using *in situ* observations. These results are consistent with the predicted accuracy of the TMI SST data products. Based on these results, a simple method to merge the TMI and ATSR data is proposed.

1. Introduction

There is now an increasing demand for high temporal and spatial resolution satellite Sea Surface Temperature (SST) data by oceanographers and meteorologists for use in operational model data assimilation schemes. Recently, the Global Ocean Data Assimilation Experiment (GODAE) high-resolution SST Pilot Project (GHRSST-PP) (Donlon *et al.* 2002a) has advocated that a new generation of SST data product should have a spatial resolution of ca 10 km and a temporal resolution of $\ll$24 hours. Due to the radiometric, sampling and spectral limitations of individual measurement systems, these demands are best met by combining datasets obtained from complementary measurement systems. The recent advances in producing SST using microwave radiometry from the Tropical Rainfall Mapping Mission (TRMM) Microwave Imager (TMI) (Wentz and Meissner 1999) are particularly important in this context. The use of passive microwave radiometers to measure SST is significant because, at these frequencies, microwave energy is insensitive to non-precipitating clouds, atmospheric aerosols and atmospheric water vapour. Their main weaknesses are poor radiometric fidelity and spatial resolution. Conversely, these are the major limiting factors of satellite infrared imagers, such as the ERS Along-Track Scanning Radiometer (ATSR), that provide high spatial and radiometric resolution SST measurements. The objective of this paper is to explore the combined use of TRMM TMI SST and ATSR/2 infrared skin SST (SST_{skin}).

*Now at MetOffice, Exeter, UK; e-mail: craig.donlon@metoffice.com

An updated version of a paper originally presented at *Oceans from Space 'Venice 2000' Symposium*, Venice, Italy, 9–13 October 2000.

International Journal of Remote Sensing
ISSN 0143-1161 print/ISSN 1366-5901 online © 2004 Taylor & Francis Ltd
http://www.tandf.co.uk/journals
DOI: 10.1080/01431160310001592256

Merging complementary data such as these requires an understanding of the characteristic differences between specific data streams.

2. The TRMM TMI and ERS ATSR/2 radiometers

The TRMM TMI instrument is similar in design to the Special Sensor Microwave Instrument (SSM/I) but has a 10.7 GHz channel suitable for retrieving SST (Wentz and Meissner 1999). Constraints on the TMI antenna diameter result in a large nadir field of view (ca 50 km) that, together with a swath width of ca 760 km, a low altitude (350 km) orbit and inclination (35°), result in extensive non-Sun-synchronous coverage of a region 40° N–40° S. A physically based retrieval algorithm (Wentz and Meissner 1997) is used to derive SST and remove the effects of surface roughness and atmospheric attenuation (primarily O_2 and water vapour) using the higher-frequency channels (19–37 GHz) of the TMI sensor.

The ERS ATSR-2 instrument is a seven-channel imaging radiometer providing skin SST measurements of unprecedented accuracy and stability (Murray *et al.* 2000) due to innovative design, including low noise detectors, continuous on-board calibration and dual view capability. It has a near-polar orbit configuration (nominal inclination of ca 98°) swath width of 512 km, a nadir field of view of ca 1.1 km and a repeat cycle of about three days. These data are then averaged into ten arc minute latitude × longitude Averaged SST (ASST) cells to provide a global SST product.

Note that the ATSR measures the skin SST, SST_{skin}, which is the temperature of the top 10–20 μm of the sea surface, whereas the TMI measures the integrated temperature of the top 1.2 mm and is believed to represent the SST at the base of the SST_{skin} layer (referred to as $SST_{sub\text{-}skin}$). Thus, comparatively these measurements are fundamentally different. However, only during low wind speeds ($<6\,m\,s^{-1}$) are significant skin deviations and warm layer effects expected to occur and at higher wind speeds the small differences may be corrected for, if required (Donlon *et al.* 1999, 2002b).

Figure 1(*a*) shows a composite of all available ATSR/2 ten arc minute average SST_{skin} data produced in the Atlantic Ocean for the evenings of the 27–29 September 1998. Figure 1(*b*) shows the $SST_{sub\text{-}skin}$ data obtained during the same period from the TMI instrument. Evening data were chosen to avoid thermal stratification that may otherwise have complicated analysis. The increase in spatial coverage provided by the TMI is considerable, although limited in latitudinal extent due to the TRMM orbit configuration: gaps in the ATSR data are due to the 512 km swath width and considerable cloud contamination associated with infrared measurements. Gaps in the TMI data are mainly due to precipitation.

3. Comparison of TRMM Microwave imager SST (v1.0) data with other observations

3.1. *Comparison with* in situ *cruise observations*

During the radiometric observations of the sea surface and atmosphere (ROSSA) 1998 experiment (Donlon *et al.* 1999), a suite of oceanographic and atmospheric measurements were made along a meridional transect across the Atlantic Ocean. Measurements included subsurface SST using a thermosalinograph (TSG) at a depth of ca 7 m (referred to as SST_{7m}) and radiometric SST_{skin} using a scanning infrared SST radiometer (SISTeR). All night-time ROSSA data coincident with TMI data were averaged across each TMI pixel using a temporal coincidence of ± 5 h. The positions of the validation data are shown in figure 2(*a*) and a comparison between the TMI and *in situ* SST is presented in figure 2(*b*).

The TMI $SST_{sub\text{-}skin}$ has a mean bias of $-0.25\,K \pm 0.7\,K$ when compared to

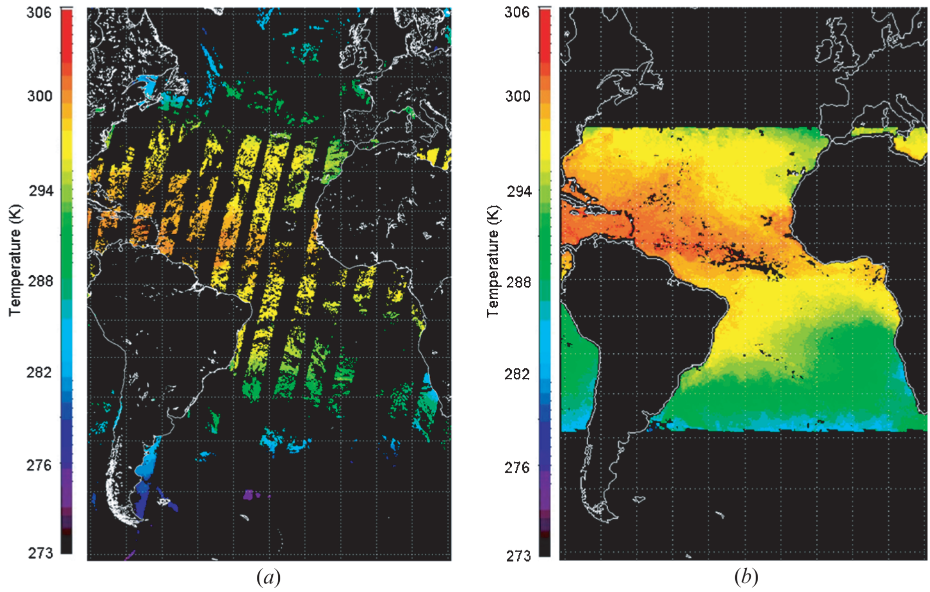

Figure 1. (*a*) ERS ATSR/2 night-time SSST for the 27–29 September 1998 (processed by the Rutherford Appleton Laboratory, UK). (*b*) TRMM TMI night-time SST for same period as (*a*) (processed by Remote Sensing Systems and available from http://www.ssmi.com).

in situ SST_{7m} (figure 2(*b*)). This bias is higher ($-0.65\,K \pm 0.7\,K$) when TMI $SST_{sub\text{-}skin}$ is compared to *in situ* SST_{skin} observations, primarily due to the mean skin temperature deviation of ca 0.3 K. Note that TMI $SST_{sub\text{-}skin}$ appears to overestimate the SST at higher temperatures, although the dataset is small.

3.2. *Comparison with ERS-2 ATSR data*

It is possible to use a reliable and well-calibrated sensor such as the ATSR (e.g. Murray *et al*. 2000) to provide a foundation for developing more advanced data characterization. For the night-time period 27–29 September 1998, all available ATSR/2 0.5° latitude × longitude cell ASST data contemporaneous to within ± 5 h with TMI SST observations were derived (ca 20 000 match-ups). A comparison between TMI $SST_{sub\text{-}skin}$ and ATSR SST_{skin} data is shown in figure 3.

These data have similar bias and rms. deviation values to the results described in the preceding section. Some of the variability is due to variations in the magnitude of the skin temperature deviation and regions of extreme surface roughness, differences due to the different spatial and temporal sampling characteristics of the TMI and ATSR instruments and the lack of exact temporal coincidence. When the difference between ATSR and TMI data was plotted as a function of meridional position (not shown), particularly 'noisy' regions could be identified, corresponding to the large precipitation regions in the Atlantic seen in the TMI data of figure 1(*b*), suggesting some rain contamination of TMI $SST_{sub\text{-}skin}$. Nevertheless, given the temporal and spatial differences and the radiometric fidelity of the TMI instrument, it is clear that the TMI is capable of providing extremely useful $SST_{sub\text{-}skin}$ data.

4. Merging of TMI and ATSR/2 SST data

The exact combination of TMI and ATSR SST, while desirable, is not straightforward because of differences in the radiometric, spatial and temporal

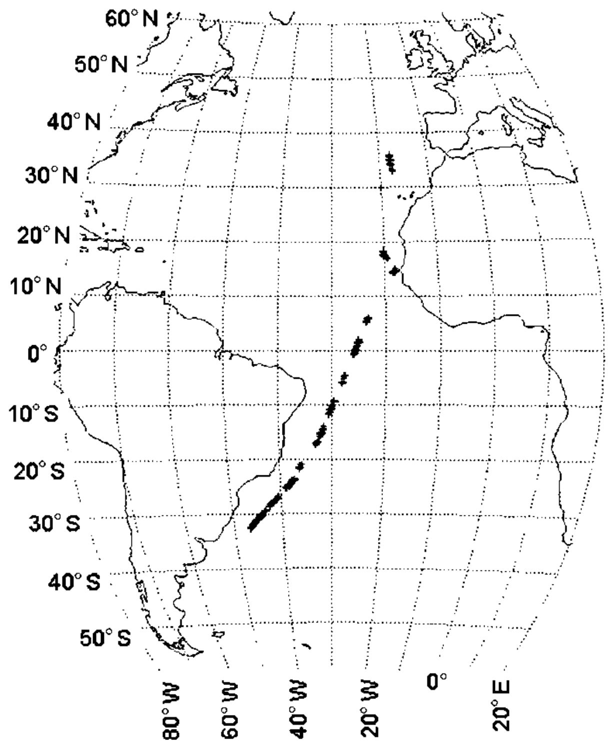

(*a*)

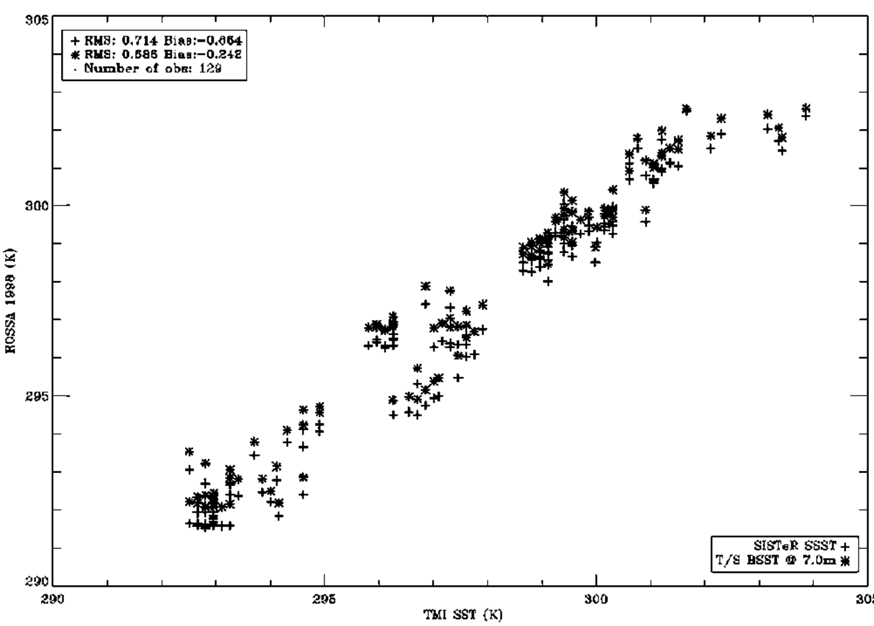

(*b*)

Figure 2. (*a*) Location of TMI pixels contemporaneous with ROSSA 1998 cruise data to within ± 5 h. (*b*) Plot of TMI SST vs. mean ROSSA 1998 SST. Comparisons between BSST @ 7 m and SSST are shown.

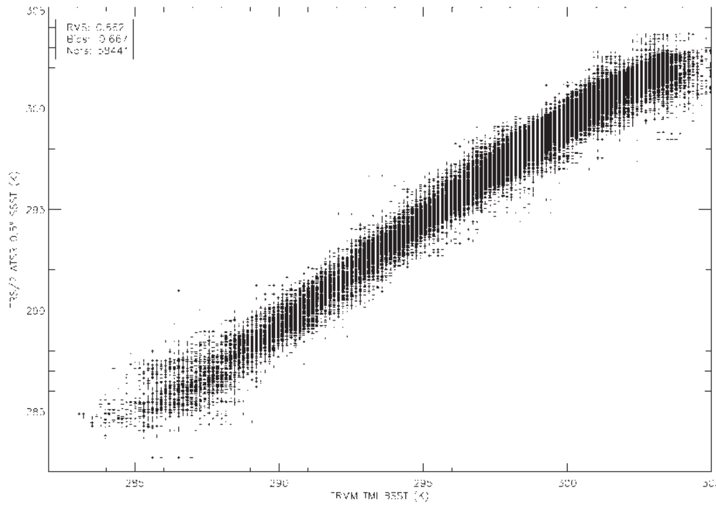

Figure 3. Night-time contemporaneous TRMM TMI SST and ERS-2 ATSR ASST data within ± 5 h for the period 27–29 September 1998.

characteristics of the instruments. However, in the simplest case, based on the comparisons discussed in section 3, the following method was used to produce a merged SST_{skin} dataset from TMI and ATSR data. TMI data are first adjusted according to the relationship shown in figure 3 (correcting for bias and the slight nonlinear relationship between the TMI and ATSR). It is assumed that the TMI SST is biased warm with respect to the ATSR data by ca 0.3 K due to the skin temperature deviation (Donlon *et al.* 1999, 2002b) and the remainder of the bias is due to TMI and ATSR algorithm differences. Finally, ATSR ten arc minute data are preserved and TMI data are mapped into the remaining ATSR ten arc minute grid using a nearest neighbour scheme. The resulting image is presented in figure 4. There are two main strengths to the method: (a) gaps in the ATSR data due to narrow swath and cloud are filled in using measurements and (b) the TMI data are 'stabilized' by the ATSR data which effectively provides a calibration data source.

5. Conclusions

In order to provide a high spatial and temporal resolution sea surface temperature dataset capitalizing on the complementary aspects of sensor-specific data streams, considerable effort to understand the characteristics of individual data streams is required. In particular, the use of *in situ* validation data is critical as it provides a measure of confidence for both the datasets used, as input to the merging methodology and to the merged output data themselves. Alternatively, it is possible to use a reliable and well-calibrated sensor, such as the ATSR, to provide a foundation for developing more advanced data fusion techniques. While the TRMM TMI instrument is pioneering microwave $SST_{sub\text{-}skin}$, sensors such as the Advanced Scanning Microwave Radiometer (AMSR) now provide improved performance due to a 6.9 GHz channel (better suited to SST measurement), and a 1600 km swath at 50 km resolution. Further development of merging complementary satellite SST datasets is required to ensure the optimal collective use of these data.

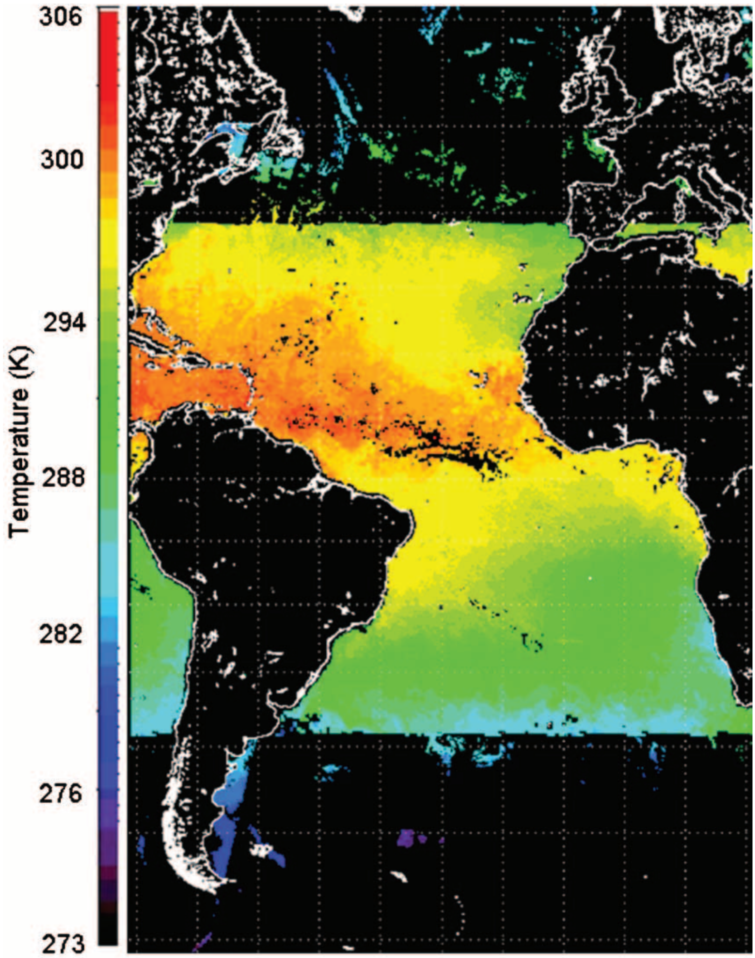

Figure 4. Combined SST_{skin} map derived from merging ATSR SST_{skin} and adjusted TMI $SST_{sub\text{-}skin}$ data for the period 27–29 September 1998.

References

DONLON, C. J., *et al* 2002a, *The Global Ocean Data Assimilation Experiment High Resolution Sea Surface Temperature Pilot Project* (GHRSST-PP: Strategy and Implementation Plan, available from the International GHRSST-PP Project Office, Metoffice, B2042, Fitzroy Road, Exeter, EX1 3PB, UK.

DONLON, C. J., MINNETT, P., GENTEMANN, C., NIGHTINGALE, T. J., BARTON, I. J., WARD, B., and MURRAY, J., 2002b, Towards Improved Validation of Satellite Sea Surface Skin Temperature Measurements for Climate Research. *Journal of Climate*, **15**, 353–369.

DONLON, C. J., NIGHTINGALE, T. J., SHEASBY, T., TURNER, J., ROBINSON, I. S., and EMERY, W. J., 1999, The Thermal Skin Temperature of the Ocean at High Wind Speed. *Geophysical Research Letters*, **26**, 2505–2508.

MURRAY, M. J., ALLEN, M. R., MERCHANT, C. J., HARRIS, A. R., and DONLON, C. J., 2000, Direct observations of skin-bulk SST variability. *Geophysical Research Letters*, **27**, 1171–1174.

WENTZ, F. J., 1997, A well-calibrated ocean algorithm for SSM/I. *Journal of Geophysical Research*, **102**, 8703–8718.

WENTZ, F. J., and MEISSNER, T., 1999, *AMSR Ocean Algorithm*, Vol. 2 (Santa Rosa, CA, USA: Remote Sensing Systems).